# An Overview of Prognosis Health Management Research at GRC for Gas Turbine Engine Structures With Special Emphasis on Deformation and Damage Modeling

**Steven M. Arnold[1], Robert K. Goldberg[1], Bradley A. Lerch[1], and Atef F. Saleeb[2]**

[1] *NASA Glenn Research Center, Cleveland, Ohio, 44135, U.S.A.*
*Steven.M.Arnold@nasa.gov*
*Robert.K.Goldberg@nasa.gov*
*Bradley.A.Lerch@nasa.gov*

[2] *University of Akron, Akron, Ohio, 44325, U.S.A.*
*Saleeb@uakron.edu*

**ABSTRACT**

Herein a general, multimechanism, physics-based viscoelastoplastic model is presented in the context of an integrated diagnosis and prognosis methodology which is proposed for structural health monitoring, with particular applicability to gas turbine engine structures. In this methodology, diagnostics and prognostics will be linked through state awareness variable(s). Key technologies which comprise the proposed integrated approach include 1) diagnostic/detection methodology, 2) prognosis/lifing methodology, 3) diag nostic/prognosis linkage, 4) experimental validation and 5) material data information management system. A specific prognosis lifing methodology, experimental character ization and validation and data information management are the focal point of current activities being pursued within this integrated approach. The prognostic lifing methodology is based on an advanced multi-mechanism viscoelastoplastic model which accounts for both stiffness and/or strength reduction damage variables. Methods to characterize both the reversible and irreversible portions of the model are discussed. Once the multiscale model is validated the intent is to link it to appropriate diagnostic methods to provide a full-featured structural health monitoring system.*

## 1 INTRODUCTION

The desire for higher performance (e.g., increased thrust to weight ratio) and efficiencies in gas turbine engines, along with the availability of advanced technologies, has resulted in designers pushing the design envelop to the limit in such areas as, for example, increasing the pressure ratio, decreasing tip clearance, and increasing operational temperatures. These advanced designs have in turn caused significant increases in overall operational and maintainability costs, due to associated uncertainties in component life and reliability. Similarly, as technology advances, component costs typically increase proportionately – thus enhancing the desire for better clarification of useful (safe) remaining life, to decrease direct operating costs. This need explains the heightened desire for and increased research activity in the area of condition monitoring with an eye toward diagnosis and prognosis of various critical components. To date, in commercial gas turbine engines continuous health monitoring is limited to generic "global" system measurements like shaft vibrations and EGT (exit gas temperatures) and localized measurements are only taken at windows of

* Steven M. Arnold et al. This is an open-access article distributed under the terms of the Creative Commons Attribution 3.0 United States License, which permits unrestricted use, distribution, and reproduction in any medium, provided the original author and source are credited.

opportunity rather than on a continuous basis. These local measurements (which involve expensive tear down) are still limited; in general, to visual/optical surface inspection techniques (measurements), which themselves fall short in their ability to detect critical defects. Conversely, in military engines which experience far more intense and often unexpected loadings, condition-based monitoring has recently been undertaken as the standard; wherein generic engine data (environment, temperature, pressure, vibration) are collected and monitored, and integrated and correlated with past mission histories. However, prognostic methodologies, as defined herein, still remain elusive, as clear linkage between damage (critical defects, life limiting events) and response signature(s), be they refined or crude, have yet to be established.

Further structural life is known to be extremely sensitive to preexistent damage such as manufacturing flaws and/or service induced damage that can cause immediate fracture or serve as sources for early fatigue cracking. Current propulsion structural life management approaches rely on a combination of predictive models and periodic inspections both on-line and off-line. The approaches primarily in use today are (Grandt, 2004): 1) Safe-Life Design - requires that the component be retired before the initiation of cracks and is susceptible to the presence of unanticipated structural or material damage that greatly reduce the crack initiation portion of the fatigue process; 2) Damage Tolerant Design - assumes a structure contains initial cracks (typically assumed equal to the largest undetected defect size), and defines the ability of the structure to resist fracture from cracks of a given size for a specified time period; and 3) Retirement for Cause - utilizes periodic inspection intervals to locate damaged components that are then either repaired or replaced. The inspection intervals are based on the time for an undetected crack to grow to fracture. All three approaches demonstrate the interdependence of diagnostic (inspection) and prognosis (life prediction) methods and stress the importance of developing the fundamental scientific causal relationships of failure to provide the key diagnostic/prognostic linkage for different material systems and structures. Large improvements in safety, life extension, and overall life cycle costs can be attained by employing a new philosophy to propulsion health management.

However, in many of the approaches currently used (Adams, 2004, Springer, 2004), the prognosis of future events is based on an extrapolation of events which have occurred previously. If the future loading is varied significantly from the previously applied loading profiles, the classical prognosis methods will not accurately predict the future response, which explains why the accuracy of these approaches is limited to only short time extrapolations. Similarly, many successes have been documented (Fatemi and Yang, 1998, Grandt, 2004) in the realm of prognosis (analytical modeling predictions); given the damage initiation site and subsequent known loading conditions. However, for truly accurate predictions of future events (that vary significantly from prior events), a physics-based prognostic model is required in which, given an initial load/damage condition, an arbitrary set of future loading profiles can be applied (in an off-line approach) to determine the future damage and ultimate life of the structure. Linkages to diagnostics methods through the use of state-awareness variables are still required, however, in order to provide information on the current load/damage state at a given point in time, so that a physics based prognostics model can independently determine the future response of the structure.

Consequently, the overall objective of the present structural health management program at NASA Glenn Research Center (GRC) (which is supported by the NASA IVHM (Integrated Vehicle Health Management) Project within the Aviation Safety Program, is to develop, implement and experimentally verify a lifing (prognosis) methodology for health monitoring of structural components operating at high temperatures, which is tightly coupled (through corresponding state awareness variables) to detection (diagnosis) techniques. In this project, NASA Glenn researchers are focusing on the development/characterization/ and experimental verification of a fully associative, physics-based, viscoelastoplastic - damage model which can be utilized as a prognostic tool within a hot structural life management system, primarily aimed at the propulsion system environment; wherein, induced localized softening mechanisms (which are strongly influenced by geometry, loading conditions, inherent defect distributions and material anisotropy) are considered. As implied above, in this work, the term prognostics refers to the ability to predict remaining life given the current state of the material. A key feature of the viscoelastoplastic model which constitutes the basis of our prognostics system is the incorporation of advanced features of the response of metallic alloys at elevated temperatures. As engine structures will encounter elevated temperatures, classical analysis methods and constitutive equations will not be able to accurately simulate the material response. The key feature of our methodology is that the time-dependent aspect of the material response (i.e., viscoelastic and viscoplastic) dominant at elevated temperatures, are accounted for within the model along with the appropriate local and global failure criteria. Therefore, the physics-based prognosis methodology proposed will be established for high temperature structural components under general loading conditions (multiaxial loading with and without overloads, cyclic effects, thermomechanical, etc.) and experimentally

validated with the design of a prognostically challenging test matrix. This test matrix will consist of bi-axial experimental demonstration problems at ambient and elevated temperatures that will be suitable for use in characterizing, evaluating and ranking prognostic (and detection) methods. While research is being conducted on both metallic and composite structures, and the overall methodology described herein is applicable to a variety of material systems, the specific results presented in this paper are focused on titanium engine components made of Ti-6-4. The general framework, once validated for the Ti-6-4 system, will be applied in the future using other prototypical alloys used in gas turbine engines, such as powder metallurgy nickel-based disk superalloys.

The paper begins with an overview of a proposed fully-integrated diagnostic/prognosis life management system, with special emphasis on how the developed prognosis (constitutive) models can fit within the proposed framework. The viscoelastoplastic constitutive model which is the basis of the prognosis framework is then described in detail. This is then followed by the efforts to date on the characterization and validation of the specific prognostic component of the proposed integrated framework. Specifically, the characterization and validation of the reversible time dependent (viscoelastic) behavior of a representative titanium alloy (i.e., Ti-6-4) is discussed as well as the current progress achieved in understanding the irreversible (viscoplastic) response. While admittedly there is significant amounts of work that have yet to be carried out so as to enable one to fully predict the deformation and damage response of a metallic structure, even the preliminary results presented herein will demonstrate the capability of the proposed prognosis model to analyze key features of the response of metallic alloys that classical analysis methods cannot capture (such as the time- and rate-dependence of the low-strain reversible response).

## 2 FULLY INTEGRATED DIAGNOSTIC/PROGNOSTIC LIFE MANAGEMENT SYSTEM (FILMS)

The life of a component is dependent not only upon its past history (i.e., the loads imposed on it, its initial and current physical condition) but also upon the future imposed loads and operating environment. Consequently, if one desires to maximize the life of a given component one must always know the current state of the component (state awareness, obtained via detection techniques), and how future events will affect its life (prognosis or life prediction), given its present condition. Given the above considerations, a two-prong approach is adopted wherein developed prognosis

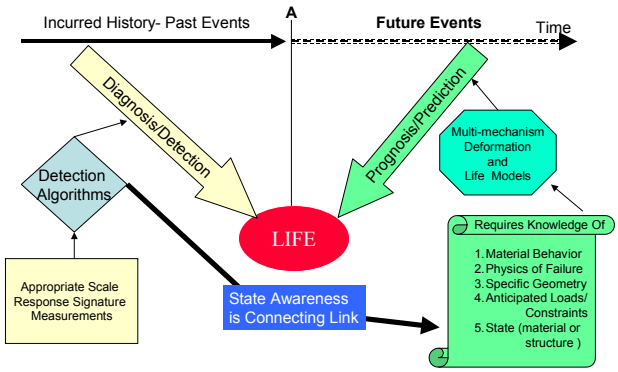


Figure 1: Depicts the distinction between Diagnostic and Prognostic Methodologies and their integration.

methods will be fully linked with complementary detection tools, illustrated in Figure 1. As discussed earlier, it is believed that only when these two views are consistently integrated (the connecting link being the current state of the material/structure) can a rational and viable health management system be established. Consequently, for the proposed prognostic model to be viable, a detection scheme (of the direct type) must be established with sufficient resolution to 1) detect the presence of defect(s), 2) locate the defect(s) and 3) size the extent of damage throughout the history of a component. Given this information, establishing a structurally meaningful connection (based on the physics of the failure or defect) with a physics-based coupled deformation and damage model is essential to predicting reliably the available remaining life given multiple future event scenarios.

Figure 2 illustrates how the diagnostic and prognostic tools need to be linked to form a full structural health monitoring system. The diagnostics tools (utilized in the "past history" portion of the chart) are required to provide the damage state at a current point in time. The prognostics tools are then utilized in the "future" portion of the chart to predict the future damage and life of the structure. As mentioned earlier, without the use of advanced prognostics tools only extrapolations of future events based on previously occurring trends (the "future=past" line in the chart) can be predicted. However, with the use of a full physics-based prognostic tool, the damage and life resulting from any potential future loading profile can be examined. Note that the "critique window" identified in the figure represents the period of time where the damage progression is examined in the structure in order to either extrapolate the future material response (in order to generate the "Future=Past" type curve) or to provide the initial conditions for a more physics-based type of prognosis methodology.

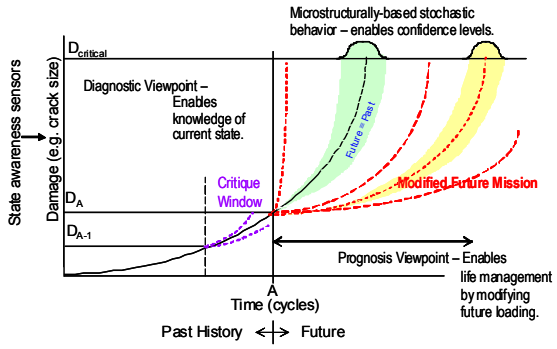


Figure 2: Depiction of an integrated diagnostic and prognosis approach to incrementally updating a life management system.

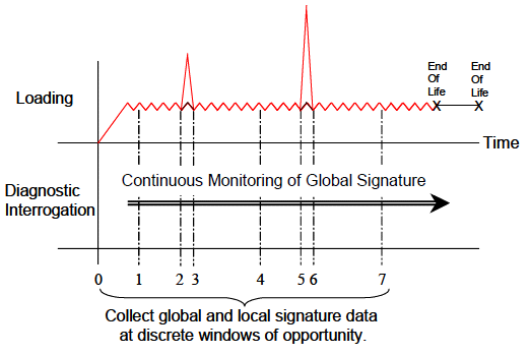


Figure 3: Temporal interrogation of a given component.

Consistent with this vision is the concept of scale-specific resolution – that is the understanding that each successive level of fidelity on the prognosis side demands a commensurate level on the diagnostic side. Consequently, many researchers have attempted to assign discriminators to allow the use of rank methods. For example, consider the four levels of damage identification (LODI) put forth by Rytter (Rytter, 1993):

- Level 1: Determination that damage is present in the structure
- Level 2: Level 1 plus determination of the geometric location of the damage
- Level 3: Level 2 plus quantification of the severity of the damage
- Level 4: Level 3 plus prediction of the remaining service-life of the structure

Note many of the popular global diagnostic techniques provide no more than LODI = 1 fidelity, when the ultimate desire is to reach level 4. Furthermore, understanding that failure is a process and not an event empowers a detection/prognosis philosophy, which can be exploited to manage the event that is developing, not just react to it. In this context, failure being a process means that the ultimate failure of a structure is due to the accumulation of damage to a significant enough degree that the structural integrity is compromised. If the initiation and progression of the lower levels of damage are not accurately detected and predicted, determination of the ultimate structural life is questionable at best. Furthermore, the higher up in the failure process hierarchy (i.e. the closer to ultimate failure) that a fault is detected, the less manageability remains and the less time exists before functionality is compromised beyond the usable state. Ideally damage should be detected well before imminent failure is present, and the prediction of remaining life should be able to take place well within the zone of safe operation, and well before the part should be removed from service. This has been referred to as the predictive horizon (Hess, 2002).

This concept is especially significant when developing a viable health monitoring system for complex "real-world" applications. In constructing such a system one must fully recognize the cornucopia of available sensor techniques and their practical limitations (e.g., inability to operate in elevated temperature environments, limited accessibility, fear that failure initiates at sensor sites, etc). Consequently, any on-line monitoring device is likely to be quite coarse in nature (i.e., scalar, e.g., pressure or EGT,) and in its spatial distribution (e.g., at very few specific locations in the engine). Alternatively, off-line diagnostic techniques are often rich in their spatial content, but ideally limited in their temporal distribution, that is, taken at intermittent windows of opportunity rather than on a continuous basis, see Figure 3. Thus the ultimate measure of success for any comprehensive health monitoring endeavor (for instance like FILMS, proposed herein) will be the ability to discriminate between these two distinct diagnostic scales (that is, a very spatially-crude but temporally-numerous versus spatially-rich but temporally-rare). Furthermore, the overarching goal must be to provide diagnostic data in sufficient quantity and quality such that the prognostic tool can make reasonable predictions.

With the above ideas in mind there are five overarching technology areas that must be addressed concurrently to establish such a robust fully-integrated, multi-scale, multi-mechanism diagnostic and prognosis life management system (FILMS). These are: 1) diagnostic/detection methodology, 2) prognosis/lifing methodology, 3) diagnostic/prognostic linkage, 4) experimental validation and 5) reasoning methodology and material data information management. In this paper, the areas of prognosis/lifing methodology and experimental validation will be concentrated on as these components will be developed in the greatest detail and most likely provide the most unique

contributions to the development of an integrated diagnostic/prognostic system. The material data information management topic will also be covered in some detail as the proper capturing, analysis, dissemination and maintaining of material data can play a significant role in facilitating the characterization and utilization of the sophisticated material model which is the heart of the proposed prognostics approach. The areas related to diagnostics and diagnostics/prognostics linkage will be described briefly, to give insight as to how the current prognostic model can be integrated within the context of a full health monitoring system. Furthermore, in the area of detection, multiple approaches (some complementary/some competitive) will be considered as resources allow as part of the research program, with an eye toward down selection and the development of a hierarchy system with varying scale specific resolution

### 2.1 Detection Methodology

Detection techniques may be classified as global or local. Global methods attempt to assess simultaneously the condition of the whole structure (e.g., vibration measurements using an accelerometer), whereas local methods provide information about a relatively small region of the system by using localized measurements (e.g., strain gages). Real-time prognosis demands a global inspection approach based on a sparse distributed network of small, efficient, environmentally stable sensors. The objective of accurate long-term lifetime prediction however, requires high levels of spatial resolution. Clearly, the two approaches are complementary to each other, with the choice of method being dependent on the scope of the problem at hand and the nature of the sensor network.

#### 2.1.1 Local Sensing/Detection Techniques

Numerous local sensing/detection techniques exist and are being studied for health monitoring applications. Some popular examples include fiber optic strain sensors and piezo-electric patches for ultrasonics. With respect to our current program, in choosing the type of detection/sensor method to be applied it is essential to fully understand the physical nature of the accumulating damage, in order to properly characterize and validate the prognostics tool. Hence, high fidelity laboratory tools will be implemented. These methods will include using a full-field optical displacement measurement system, thermoelastic stress analysis, as well as distributed strain gages. Field-friendly approaches will include passive (i.e., modal acoustic emissions) and active ultrasonics (e.g., guided wave, nonlinear, etc.). Although the high fidelity tools are not intended for field use, they define the upper limits of material assessments. The resulting database will allow for the benchmarking and capability assessments of the innovative sensors being studied within the IVHM project.

#### 2.1.2 Global/Hybrid Detection Techniques

There are basically two approaches for mathematical representation and implementation of global detection techniques, i.e., system-identification and direct post-processing of measurement data. The two approaches differ mainly in the amount and type of information used. In one extreme, the system identification approach is typically based on a complete analytical model that is optimally fitted to the measured response. Consequently this indirect approach has traditionally been restricted to numerical simulations of linear systems. Another disadvantage of this type of approach, in addition to the intense computational demands, is the need to treat the "inherent non-uniqueness" of measured data. However, more recently, novel indirect detection techniques utilizing such indicators as weighted and mixed transmissibility functions and nonlinear dynamic behavior in both the healthy and damaged systems have been emerging. Their advantage stems from their insensitivity to boundary-condition and other system nonlinearities (which can typically mask damage in most diagnostic features or otherwise cause false-positive alarms), their ability to use distributed sensor arrays to locate damage, and their applicability for "passive" diagnostics when input measurements are unavailable or environmental fluctuations are anticipated. Conversely, direct-detection schemes do not require a priori identification of an analytical model. Instead, the key ingredient is the selection of an appropriate damage index that is sufficiently sensitive to perturbations in system properties. Given this damage index, the whole implementation reduces to a pattern-recognition problem. Processed experimental data yields a signature that is compared to the base or reference state. Clearly, sharper resolution will be obtained with more distinct differences between two signatures – thus the need for robust NDE (local) techniques; e.g., see further elaborations in Saleeb and Ponnaluru (2006), Saleeb and Prabhu (2002).

In light of the above comments, this program will concentrate on utilizing full-field strain measurements as well as obtaining a variety of other detection signatures that can be utilized to evaluate both direct and indirect global detection schemes. Their determination of the material or structural condition will then be used in the companion prognosis tool to assess useful remaining life given various future event scenarios. Furthermore, the information derived from these direct and indirect global detection techniques will be used to guide the detailed local inspection

techniques discussed above to accurately quantify the specific type of damage state induced, and to improve the accuracy in subsequent life prediction calculations.

### 2.2 Prognosis Methodology

A prerequisite for meaningful assessment of component durability and life, and consequently design of structural components, is the ability to accurately predict stresses, strains, failure modes and their subsequent interaction and evolution occurring within a loaded structure, composed of a given material. Furthermore, since constitutive material models provide the required link between stress and strain, this by necessity demands an appropriate constitutive behavior model for any material (be it monolithic or composite) before that material can be certified for use by a designer Also, it is clear that the ability to identify the proper failure modes lies largely in the accurate stress-strain predictions resulting from constitutive models and their interaction with the evolving damage or failure state. Further complicating matters, the mechanisms which induce localized softening (i.e., local inelasticity, nucleation and growth of damage (defects, voids, cracks, etc.)) and ultimately lead to end of useful component life are strongly influenced by geometry, loading conditions, inherent defect distributions (e.g., those due to manufacturing) and environmental conditions. Consequently, it is virtually impossible to predict the location of failure without a complete knowledge of the initial distributions of inherent (e.g., manufacturing) flaws. Hence, people are motivated to turn to non-destructive evaluation techniques to quantify these flaws and to probabilistic approaches to account for uncertainties. Note, however, that in general the level of these uncertainties will change in time due to the path-dependent nature of deformation, internal stresses and damage evolution throughout a component's useful life; thereby making a purely probabilistic approach insufficient for a complete formulation of a prognosis framework. Yet the possibility that information can be gleaned from an intermittent diagnostic interrogation of the material still exists and thus could provide the vital link to complete the ultimate overall prognosis framework. These facts illustrate the major disadvantage of a purely prognosis approach – that is, the accuracy of life prediction is dependent upon the knowledge of both constitutive behavior of the material that comprises the structure and knowledge of the applied loads and boundary conditions.

With the above facts in mind, we have decided to evaluate a physics-based, multi-mechanism viscoelastoplastic deformation model coupled with continuum-based stiffness and strength degradation damage parameters as a prognosis methodology under general loading conditions, which will be described in much more detail in Section 3 of this paper. Although this model represents the current state-of-the-art in the area of prognosis, it is still presently not up to the challenging task of providing a complete prognosis tool; as a direct and useful complimentary diagnostic technique that links the current "material state" via state-awareness variable(s) (e.g., stiffness and strength reduction parameters) that implicitly dictate failure is still lacking. However, as the characterization, validation and demonstration of the constitutive model is a vital first step in the development of the health monitoring approach, the full development of the prognosis methodology is the current focus. The status of this methodology development effort will be further discussed in Sections 3-5.

### 2.3 Diagnostic/Prognostic Linkage via State Awareness

As stated previously, it is virtually impossible to accurately predict the location of failure without a complete knowledge of the spatial (e.g., location, origin, size) and temporal distributions of inherent and load-induced flaws – thus the need for robust global and local diagnostic tools. Similarly, component life is known to be dependent upon accurate stress-strain predictions, which in themselves are strongly influenced by the triggering and evolution of softening mechanisms (which, in turn, are heavily influenced by component geometry, loading conditions, inherent defect distributions and environmental conditions). Consequently, intermittent communication of the diagnostic material state is needed to guide and drive the predictive prognosis capability. It is our strong belief that this linkage constitutes the most innovative, and yet challenging, aspects of structural health monitoring. Interestingly, this linkage is the most coveted and yet least mature and therefore has the highest risk associated with its development. However, the state awareness approach has been considered previously. The primary challenges for our work will be to develop state awareness methods which provide the specific inputs required for the advanced prognostics constitutive model described in Section 3 of this report. Two different approaches will be investigated (as resources allow) in the future. Firstly, a "direct" identification of a spatially higher-order state awareness variable(s), representing the salient features of the changing condition of the material or structure, needs to be identified to characterize the precise nature of the damage sustained. Secondly, recognizing that (even with the advanced nature of the analysis employed) a complete and totally reliable characterization of all of the possible modes of damage is unlikely, thus a probabilistic framework will

ultimately need to be developed in the future to quantify the likelihood a given set of detection system outputs correspond to a particular type of damage. The full development and verification of the prognostics model to be described in Section 3 of this paper (particularly the damage prediction features), and the planned corresponding experimental subcomponent demonstration work described in Section 2.4 must be carried out before the efforts described here can be fully completed. However, the following discussion indicates how the prognostics tool will be coupled with appropriate diagnostics tool, and features that will be paid particular attention in the final development of the constitutive model.

### 2.3.1 Direct State-Variable Awareness Approach

The mechanical deformation results and the diagnostic signatures (both global and local) which will be coming from a series of in-plane biaxial experiments (to be described later in this paper) will be employed to:

1) Identify the type of damage (general flaw/defect/degradations) and its structurally significant manifestation (e.g., loss of stiffness, strength reduction, and/or increased damping to name a few).

2) Quantify (mathematically) the associated state-awareness variable, that is, a scalar, vector or tensor type variable(s). We anticipate the conclusion will be that the required state variable(s) will be higher-order in character (i.e., non-scalar) since they must ultimately account for the collective arrangement of multiple locations of defects that vary in size and are anisotropically oriented. Key issues will be;

a) How do we obtain these values from measured signatures?

b) How are the obtained values associated with one or more of the included damage variables (i.e., the stiffness reduction and/or strength reduction variable) within a continuum based prognosis method so that the prognosis calculations are impacted by the evolution of damage (e.g., growth of crack(s)) and/or these state variables?

c) What LODI is desired?

Clearly the outcome is far from straight forward, nor is it independent of the type of damage being tracked. Selection will be made with an eye toward feature extraction and elimination of the inherent deficiencies in the diagnostic measurement. For example, frequency measurements may be sufficient for level 1 (indicating the presence of damage) but will not let one move to LODI levels 2 through 4, due to their scalar nature.

3) Characterize the damage and state awareness variable (e.g., crack length) and its evolution; and associate it with the corresponding failure mechanism (fatigue crack) and its evolution.

Address the statistical variation in measurements and impact on the prognosis methodology.

4) Develop an updating scheme so that intermittent and/or continuous diagnostic information (state awareness) can and will impact the prognosis algorithm.

a) The scheme must address the level of measurement and analysis fidelity required both spatially and temporally to achieve the desired LODI.

b) Perform sensitivity studies to identify the level of error or uncertainties.

## 2.4 Experimental Subcomponent Demonstration

A key aspect of any credible life management system is an experimental demonstration. To properly characterize a material, a set of experimental characterization and validation tests need to be conducted, both at coupon and subcomponent levels. Uniaxial coupon tests are required in order to fully characterize the time dependent reversible and irreversible deformation and damage response of the material. For example, to characterize a metallic material using the viscoelastoplastic model described later in this paper, an extensive series of tensile, creep, relaxation, step and cyclic tests need to be performed at a variety of loading rates and temperatures. Examples of the processes used to characterize a representative titanium alloy will be described and demonstrated in detail later in this paper and are also discussed in (Saleeb et al., 2001; Saleeb and Arnold, 2001; Arnold et al., 2001; Saleeb and Arnold, 2004).

However, in order to fully investigate the crack propagation resulting from realistic multiaxial loading conditions, and to allow for the full validation of the prognostic tool, in-plane biaxial plate testing (at both room and elevated temperature) will be the primary focus of the experimental validation effort after the uniaxial characterization and validation processes are complete, so that a variety of high quality diagnostic measurements (signatures) including full field displacement and strain measurements can be successfully made. The availability of such accurate measurements, both spatially and temporally, are essential in providing validation data for the prognostic tool, but also to provide the prerequisite information for

defining an appropriate state-awareness variable(s) and their associated diagnostic technique(s). A further benefit to concentrating on biaxial plate testing is the large number of "static" structural applications that will be impacted because of the resulting enhanced level of understanding; for example, wings, nozzles, inlets, ships, tanks, etc. This list is further extended when one factors in that both room temperature and elevated temperature biaxial testing will be performed; thus allowing the study of material nonlinearity effects, which are present in many of the targeted applications, and the simulation thereof is a specific strength of the constitutive model which comprises the prognostic tool. Although the specific test matrix has not be finalized to date, Table 1 outlines a proposed matrix that illustrates both the spirit and thought process, which will embody the final test matrix. In keeping with our two-prong philosophy of both developing prognostics methods and accompanying diagnostics techniques, we have chosen to construct an in-plane test program along two lines; variation in imposed load history and inflicted defect configurations. In this way, assessment of both local and global NDE techniques (in the context of associated state awareness variable(s)) and the selected prognosis methodology can be readily achieved.

The baseline plate configuration to be examined will be the classic problem of a plate with a single stress riser (e.g., a hole) loaded uniaxially and biaxially under both monotonic and cyclic histories. This baseline case will be complimented by two other configurations with multiple stress risers of varying character (i.e., holes, slots, cracks, etc.), which might correspond to inherent structural attachment configurations and/or large scale structural damage.

The variety of crack initiators will be examined with an eye toward developing a significant database to characterize and validate the proposed life management system under relatively realistic conditions and to enable assessment of the uncertainties in the underlying failure mechanisms. Figure 4 (top) illustrates the baseline (B) configuration which, when combined with the specified load histories in Table 1, will become prognostically challenging (PC) problems. The second configuration, a center hole surrounded by a symmetric pattern of smaller holes, (see Figure 4 (middle)) is considered to fall into the category of diagnostically challenging (DC) due to the inherent non-equal excitation intensities around the inflicted defects. Additionally, this configuration is anticipated to be prognostically challenging. The third configuration, a center hole with other multiple damage sites with varying character (location, size, geometry, sharp, smooth, etc.), is considered to be both diagnostically and prognostically challenging (DPC), irrespective of the applied load history and will thus be used primarily for validation/demonstration of the developed life

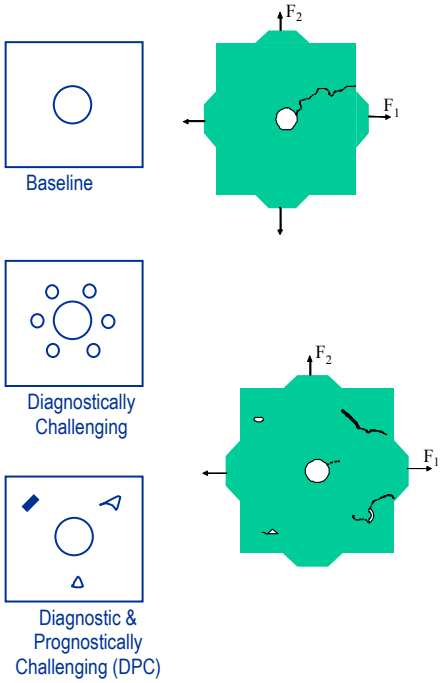


Figure 4: Schematic of biaxially loaded plate with various inflicted defect configurations.

Table 1: Test Matrix for Biaxial Test Program

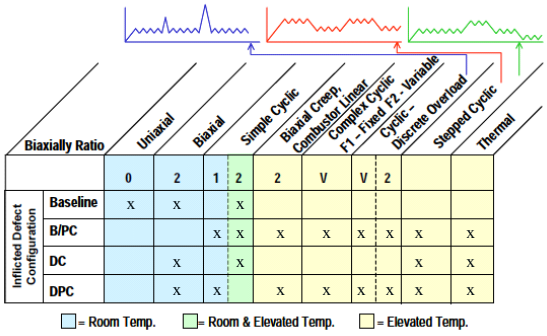


management system. Furthermore, a number of these tests will actually be performed "blind", i.e., the inflected damage state will be kept hidden from the analysts during the verification process in order to fully verify the developed approach.

With respect to imposed load history, a number of biaxiality ratios (BR = F1/F2) are anticipated: for example BR = 0 (uniaxial), BR=1 (equal biaxiality – pressure sphere), BR = 2 and/or 0.5 (representing that in a cylindrical pressure vessel such as a combustor liner) and lastly a varying ratio, BR=V, wherein one component is held fixed while the other is varied. Although monotonic load histories will be imposed, emphasis will be placed on fatigue induced cracks, with more complex histories involving thermal cycles,

periodic overloads, and stepped histories being conducted for validation at later stages of the research program. Consequently, initially room temperature BR=0,1,2 monotonic and simple cyclic histories (see light blue cells in Table 1) will be conducted so as to enable state-awareness characterization, diagnostic down-selection and prognosis enhancements. The remainder of the tests in Table 1 are to be conducted both at room and elevated temperature (see yellow and green cells in Table 1).

A key aspect of this experimental program will be the precise documentation of the order (both temporally and spatially) of flaw insertion (be it operator and/or load history induced) thus enabling appropriate interrogation of the data (i.e., diagnostic signature and deformation and life - structural manifestation) to assess both sides of the proposed life management system, i.e., Figure 1. For example consider the following envisioned test procedure:

1) Obtain material property and uniaxial response curves required by the viscoelastoplastic prognosis model.

2) Perform flat plate characterization tests: Fully known conditions with a single stress riser (see Figure 4 (top))

a) Apply all desired diagnostic techniques to "virgin" plate (no hole)

b) Induce hole of specified diameter, location and character (thus overwhelm any inherent defects/flaws due to manufacturing) - again apply all down selected diagnostic techniques to the plate.

c) Mechanically load plate and monitor initiation and propagation of crack(s) by taking a variety of spatial (full-field, and discrete location) measurements (strain-based, vibration and all other selected diagnostic techniques) at various time intervals (intermittent and continuous) throughout the mission profile, see Figure 4 (middle).

Steps a, b, and c for different load histories would be repeated. In the case of validation tests (i.e., when multiple stress risers (see Figure 4 (bottom) are present) the above steps will be used except for the insertion of the following step d in between steps b and c:

d) Impose predefined defects (with specific character) at specified locations; obtain all signatures. This will simulate material randomness in that multiple initiation sites can occur at unexpected locations when a mechanical load is applied, thus challenging both diagnostic and prognosis methodologies.

The results will thus enable the quantification of detectibility sensitivities in the state-awareness variable(s) and prognosis methodology characterization. Given the above-generated data, we hope to be able to answer the following questions:

i) Can we detect the presence, location and character (size, geometry, nature) of a defect be it operator or history induced.

ii) Can we detect/predict when and where damage (crack) initiates (criteria specific) and how and at what rate does it propagate within a plate given a biaxial load history.

Note the presence of a variety of stress risers will provide the required randomness to validate both diagnostic and prognosis aspects, as well as allow linkage/ connection between them to be established.

iii) What are the appropriate state awareness variables for this type of damage mechanisms?

iv) What is the remaining life of the plate at any given time and how should one modify the load to maximize remaining life.

v) What level (fidelity) and type of detection signatures are required to provide a specific confidence level of prognosis (criteria specific)?

### 2.5 Material Data Information Management

To properly characterize and validate the constitutive model at the heart of the prognostic tool, the ability to capture the fundamental response data (i.e., the entire uniaxial/multiaxial response curve with its full pedigree, chemistry, processing, heat treatment, testing information, etc.) and application potential of a given material system and not just specific predefined (generally accepted point wise) values is required. Furthermore, as knowledge evolves these and other yet unmined data need to be processed and linked thereby becoming information and ultimately knowledge. Furthermore, although specification of typical test matrices involve, either explicitly or implicitly, *a priori* selection of a modeling approach; to maximize the value of any given experimental program (for both present as well as yet to be developed models) one must attempt to capture and document as much material response information as possible without prejudice to any particular model (idealization).

This general data, information, knowledge pyramid is at the core of the material data life cycle (see Figure 5a) proposed by the Material Data Management

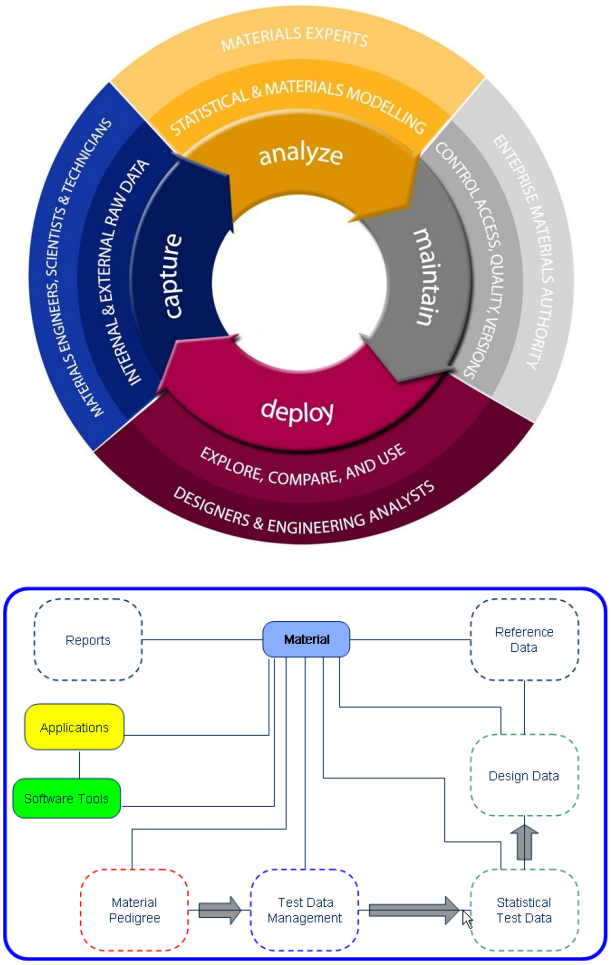


Figure 5: (a) Four aspects of material data lifecycle and (b) schematic illustrating a possible data schema for the material information.

Consortium (MDMC) (MDMC, 2006), wherein data is captured and consolidated from external sources, legacy databases as well as internal (possibly proprietary) testing programs. Next, data is analyzed and integrated to create or discover useful information and then disseminated to the people who need and use it. The continual maintenance of the whole system (the data and information generated as well as the relationships, or links, between them) becomes the last yet essential stage of the data life cycle. Note that the middle ring of Figure 5a provides additional information regarding the type of data utilized and functions performed during each phase in the data life cycle; while the outer most ring details the individuals most likely responsible for these functions.

To support the various required activities throughout this data life cycle requires the (preferably seamless) integration of a variety of software tools. These range from data input, reduction/analysis, visualization, reporting tools; material parameter estimation tools; product life management tools (PLM); to structural analysis codes that utilize a central database. These tools should enable material and structural engineers to input, manage and utilize information in as an efficient, reliable and user-friendly way as possible. Finally, these tools should also enable enterprise-wide (even world-wide) solution or access.

A possible material database schema at a very high level illustrating a portion of the information contained and its associated linkage within this centralized database is depicted in Figure 5b. Note that within each dotted area a number of lower level data tables would be grouped. For instance within the Test Data Management area, one would find data tables for each category of test data (i.e., tensile, creep, relaxation, cyclic, crack growth, etc.) wherein each individual record would contain both generally accepted point values and the complete response histories for each individual test along with images of failure surfaces and microstructures. Within the Statistical Test Data section, one would find the corresponding consolidated (statistically combined) response of a given material for each test category of interest. Finally, after further consolidation and characterization of company- specific algorithms and life modes, the corresponding material design allowables (e.g., stress, strain, elongation, etc.) would be stored for each material of interest. Such information storage and linkage enables full traceability of each and every data item.

## 3 COUPLED MULTIMECHANISM VISCOELASTOPLASTIC DEFORMATION AND DAMAGE MODEL

As discussed earlier, a key concept in the FILMS methodology, described previously, is the linkage of an advanced constitutive model used for prognosis with an accompanying diagnostic system. Due to its vital role in the overall structural health management approach the development, characterization and validation of a unified, coupled deformation and damage constitutive model is the current focus in this research program due to resource limitations. The primary tool for carrying out the prognosis methodology is a multiscale framework depicted in Figure 6 which includes a set of constitutive equations known as the GVIPS (Generalized Viscoplasticity with Potential Structure) model (Arnold and Saleeb, 1994; Saleeb et al., 2001; Saleeb and Arnold, 2001; Saleeb and Arnold, 2004). This model is a complete (fully associative) potential framework wherein strain, stress, and the thermodynamic functions (stored energy and dissipation), have been appropriately partitioned to form a general viscoelastoplastic, multimechanism, deformation and damage model. This GVIPS

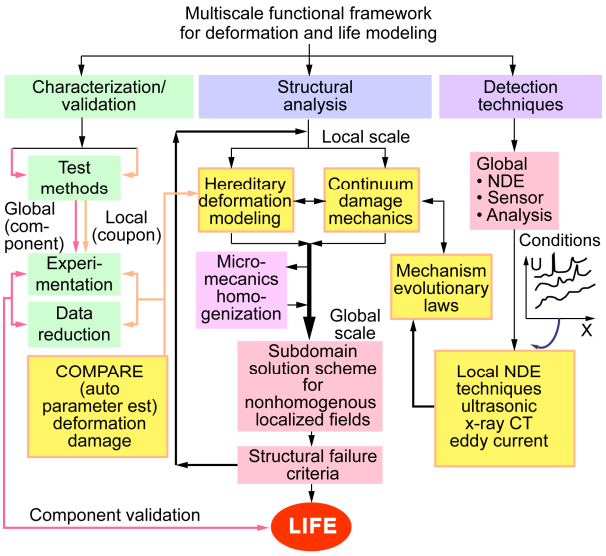


Figure 6: Multiscale framework describing the interaction between experimentation, analysis and detection techniques to enable accurate deformation and life modeling.

framework attempts to simulate the underlying physical processes associated with microscopic defects (e.g., dislocations, grain boundaries, voids, etc. in metals) and their complicated interactions which span an entire spectrum of length scales (i.e., from the "atomistic (nano) -- microscale", to the "mesoscale" to the final "macroscale") by introducing the notion of multiplicity of mechanisms in the mathematical description. Consequently, the complex nonlinear, time-dependent deformation and damage response of any metallic structure can be analyzed using this framework.

As the model can be applied in making off-line predictions of the deformation, damage and life of a structure given an arbitrary loading history, as well as within an on-board prognostics system where a given set of current damage parameters and load states measured by sensors and lined by state-awareness methods, could be utilized for predicting the damage progression and life of a structure accounting for any number of possible future loading scenarios. Also, as will be elaborated on shortly, the strength of this particular modeling approach is its ability to fully account for the time- and rate-dependence and nonlinearity of the material response, and their interactions, in both the reversible and irreversible regimes, in ways that classical plasticity and creep analysis methods cannot.

The mechanisms referred to above, reflecting the vastly different interactions in the material microstructure, give rise to the introduction of an aggregate of individual internal state variables (i.e., $q_{ij}$, $\alpha_{ij}$, $\theta$, and $\psi$, see Figure 7); e.g. many tensors each accounting for interactions at different length scales, that is, "short" range (atomistic movements such as climb and diffusion), and "long" range (dislocation movement, subcells and grains). In addition to the differences in "microstructural" length scales, the time rates of change governing their dynamics are also known to be vastly different, hence the notion of multiple (or spectrum of) characteristic relaxation times in the GVIPS formulation, i.e., $M_{ijkl}$ and $\eta_{ijkl}$ , see Figure 7.

Furthermore, with energy measures providing the major consideration in dislocation dynamic theories (e.g., in studying thermal activation, mass and vacancies diffusion, energy barriers such as jog formation energy, rate-dependent and multi-species (distributions of finite-strength obstacles, etc.)) and the intricate interaction of such "unit" processes, with their vastly different energy contents and rate-limiting values, the partitioning of the overall supplied work into energy storage (e.g., hardening) and energy dissipation (e.g., recovery and inelastic flows) components that proceed with varying degrees of competition during the deformation of the material became a motivating factor. Hence the emphasis on a complete-potential "energy" structure which leads to a "hierarchy" of representations, from the Gibb's ($\Phi$) and dissipation ($\Omega$) functions (grandparent), to the kinematic decomposition of the deformation and microstructure state equations (parent), to the kinetic and evolution equations (children). This structure then guarantees i) that the overall response is always bounded in terms of the total and/or rate quantities (e.g., transient to steady-state creep, or from a state of nonlinear hardening to a state of saturation in hardening) and ii) the availability of symmetric tangent stiffness matrices which greatly enhance computational robustness. Finally, the use of multimechanisms (embedding the effects of many time/length scales) in the GVIPS class of formulation enables the specialization of this general model into simpler, and more restricted in scope, formulations, e.g., purely elastic, linear viscoelastic, classical rate-independent elastoplastic, as well as more elaborate forms of hereditary descriptions (involving viscous effects, nonlinear hardening, dynamic recovery, thermal/static recovery, relaxation, ratcheting or shakedown phenomena under load cycles) to name a few. More recently (Saleeb and Wilt, 2005), this formulation has been extended to include two types of damage measures, that is, strength and stiffness reduction. In the case of irreversible material softening strength reduction, each of the hardening functions $h_b$ are degraded separately by the scalar $\theta^{(b)}$, which is the measure of the amount of strength reduction damage for each mechanism (b), and varies from 1 to $\infty$ (1 denoting the undamaged ("virgin") state and $\infty$ the

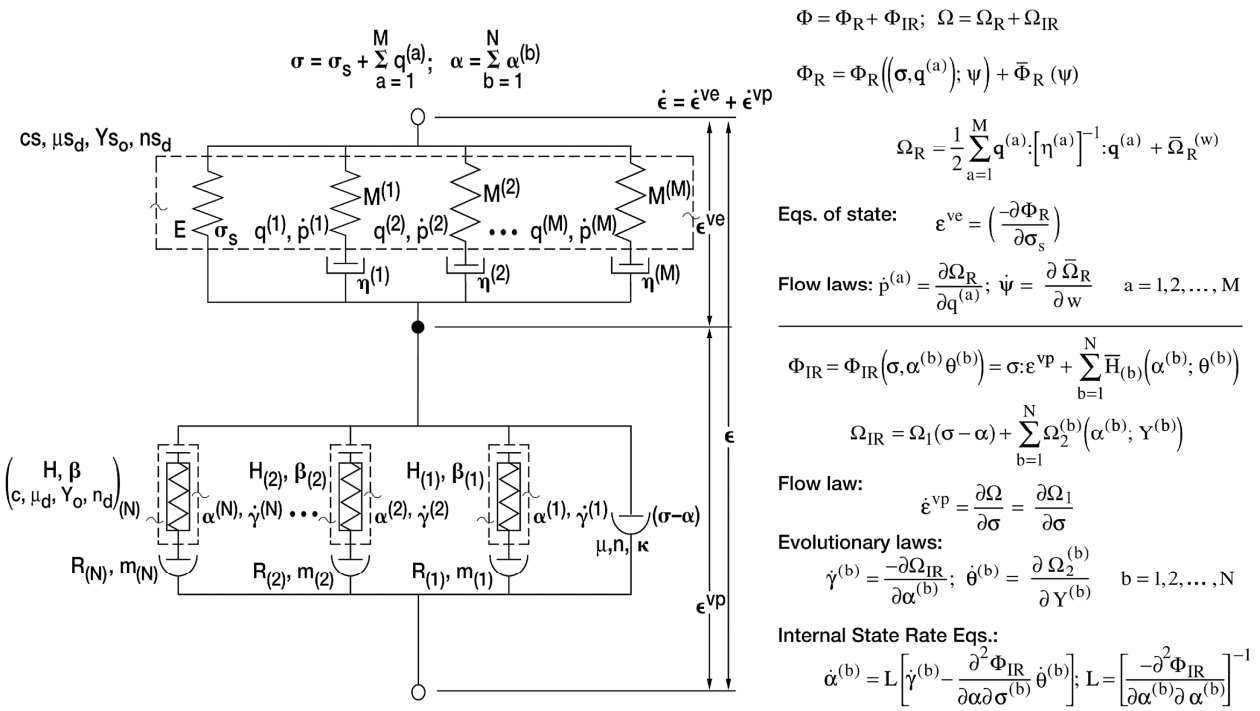


Figure 7: Analog representation of multi-mechanism deformation and damage GVIPS framework with key governing equations.

fully damaged state). Consequently, a new associated pair of conjugate state variables $Y^{(b)}$ and $\theta^{(b)}$ (stress- and strain-like, respectively) whose time evolutions are given in terms of the total hardening stored energy of plasticity (i.e., plastic energy release $Y^{(b)}$) for the corresponding mechanism, b are introduced. On the contrary, for softening due to material stiffness degradation, the entire viscoelastic moduli tensors $E_{ijkl}$ and $M^{(a)}_{ijkl}$ are degraded simultaneously by the scalar damage parameter $\Psi$, where $\bar{Y}$ and $\Psi$ are the new conjugate (stress- and strain –like, respectively) set of stiffness- damage state variables. Note, the quantity $\Psi$ is the measure of the amount of stiffness damage and varies from 1 to $\infty$ (1 again denoting the virgin undamaged state and $\infty$ being the fully damaged material). It is important to note that the evolution of damage is directly evaluated and does not require any iterative updates in the implicit integration scheme for the other stress and internal variables. In the present model, a single stiffness damage mechanism (identified by the dotted line in the reversible strain region, i.e., the upper region, of Figure 7).

Although the GVIPS class model inherently represents numerous distributed defects (dislocations /micro /meso/ macro cracks) and their interaction phenomenologically, and has the potential for tackling the problem of damage evolution from localization to final macro failure, it currently lacks a reliable criteria for tracking such intricate evolution (i.e., macro-crack initiation and propagation (branching, kinking, etc.)) of damage as expected in realistically loaded structures. Providing these criteria, associating the above damage variables with appropriate state-awareness variables and demonstrating the ability to predict life accurately will be the focus of the next steps in the project, i.e., establishing the state awareness linkage between the prognosis and diagnosis methods, after the initial characterization and validation of the base material model is complete. Note, the time dependent aspect of the model (i.e., viscoelastic and viscoplastic) will primarily dominate at elevated temperature; while room temperature typically allows significant simplification to be made within the model. However, as will be described in somewhat more detail subsequently, the ability of this model to analyze the key time-dependent aspects of the material response at elevated temperatures represents a significant advantage of the modeling method over classical approaches. As this general, multi-mechanism, hereditary deformation and damage model has been shown to accurately represent a wide spectrum of material responses under different loading conditions for the case of titanium alloys (Arnold et al., 2001; Saleeb et al, 2001; Saleeb and Arnold, 2004). Examples include 1) rate-dependent (effective) material tangent stiffness during initial loading or any subsequent reversed loading, 2) pure

transient response (e.g., in creep or relaxation) within the reversibility region, 3) anelastic behavior upon stress reversal, irrespective of the load level, as well as, 4) other response features common to 'unified viscoplastic' formulations (e.g., rate-sensitivity, creep-plasticity interaction, thermal recovery, etc.).

To describe the GVIPS model in more detail, we begin with a key assumption of the additive decomposition of the total strain tensor, $\varepsilon_{ij}$,

$$\begin{aligned} &\varepsilon_{ij} = \varepsilon_{ij}^{ve} + \varepsilon_{ij}^{I} + \varepsilon_{ij}^{th} \\ &or \\ &\varepsilon_{ij}^{ve} = \varepsilon_{ij} - \varepsilon_{ij}^{I} - \varepsilon_{ij}^{th} \end{aligned} \tag{1}$$

into three components; that is a reversible mechanical strain, $\varepsilon_{ij}^{ve}$, (i.e., elastic/viscoelastic); an irreversible strain, $\varepsilon_{ij}^{I}$, (i.e., inelastic or viscoplastic); and a reversible thermal strain, $\varepsilon_{ij}^{th}$ component. Numerous models describing the evolution of the inelastic strain have been proposed in the literature (Dowling, 1999; Lemaitre and Chaboche, 1990; Skrzypek and Hetnarski, 2000; Odqvist, 1936). Here we will utilize the GVIPS model, including its more recent extension into the coupled deformation and damage regime (Saleeb and Wilt, 2005), which has been formulated with sufficient generality to permit systematic introduction of multiple mechanisms.

The following generalized anisotropic, coupled deformation and damage material behavior constitutive model to provide for both viscoelastic (time-dependent reversible) and viscoplastic (time-dependent irreversible) response components ; where there are 6+ 2M reversible constants (i.e., $E_s$, $M_{(a)}$, $\nu$, $\rho_{(a)}$, $c_e, \overline{Y}_0, \mu_e, n_e$ ) and 3+9N irreversible constants (i.e., $\kappa$, n, $\mu H_{(b)}$, $R_{(b)}$, $m_{(b)}$, $\kappa_{(b)}$, $\beta_{(b)}$, $c_d^{(i)}, Y_0^{(i)}, \mu_d^{(i)}, n_d^{(i)}$ ) where M is the number of viscoelastic and N defines the number of viscoplastic mechanisms.

$$\dot{\sigma}_{ij} = \mathrm{E}_{ijkl}\left(\dot{\varepsilon}_{kl} - \dot{\varepsilon}_{kl}^{I}\right) + \dot{q}_{ij}\,, \tag{2}$$

$$\dot{q}_{ij}^{(a)} = \mathrm{M}_{ijkl}^{(a)}\left(\dot{\varepsilon}_{kl} - \dot{\varepsilon}_{kl}^{I}\right) + \mathrm{M}_{ijkl}^{(a)}\eta_{klrs}^{(a)-1}q_{rs}^{(a)} - (\Psi - 1)\sigma_{ij} \tag{3}$$

$$\dot{\varepsilon}_{ij}^{I} = \begin{cases} f(F)\Gamma_{ij} & \text{if } \mathrm{F} \geq 0, \\ 0 & \text{otherwise,} \end{cases}; \tag{4}$$

$$\dot{\alpha}_{ij}^{(b)} = Q_{ijkl}^{(b)}\left[\dot{\varepsilon}_{kl}^{I} - \frac{R_{(b)}\left[G^{(b)}\right]^{n_{(b)}}}{H_{(b)}\left\langle 1-\sqrt{G^{(b)}}\right\rangle^{\beta_{(b)}}}\pi_{kl}^{(b)} - (\theta^{(b)}-1)\pi_{kl}^{(b)}\right] \quad \text{if } \pi_{kl}^{(b)} - (\sigma_{kl} - \alpha_{kl}) \geq 0 \tag{5}$$

where,

$$Q_{ijkl}^{(b)} = H_{(b)}\left\langle 1-\sqrt{G^{(b)}}\right\rangle^{\beta_{(b)}} \times \left[Z_{ijkl} - \frac{\beta}{2\kappa_{(b)}^2\sqrt{G^{(b)}}\left[1-\{1-\beta\}\sqrt{G^{(b)}}\right]}\alpha_{ij}^{(b)}\alpha_{kl}^{(b)}\right]$$

Note $Z_{ijkl}$ is the "generalized" inverse of $\Lambda_{ijkl}$; see (Saleeb and Wilt, 1993); for further elaboration on this. Next the evolution of stiffness degradation is governed by

$$\begin{aligned} &\dot{\psi} = c_e\,\overline{\dot{Y}} \\ &\overline{\dot{Y}} = \frac{1}{\mu_e}\left[\left(\sqrt{\dot{\varepsilon}_{ij}\dot{\varepsilon}_{ij}}\right)^{\frac{1}{ne}} - \frac{1}{\overline{Y}_o}\right] \end{aligned} \tag{6}$$

when the current magnitude of the total strain ($\overline{\varepsilon}$) is greater than a cut-off value ($\overline{\varepsilon}_{\text{cut}}$) below which no damage accumulates, i.e., $\dot{\Psi} = 0$. Similarly, if the current magnitude of the inelastic strain is above a given cut off value ($\overline{\varepsilon}_{\text{cut}}^{\text{I}}$) the evolution of the strength reduction damage variable(s), $\theta^{(b)}$, becomes:

$$\begin{aligned} &\dot{\theta}^{(b)} = c_d Y^{(b)} \\ &\dot{Y}^{(b)} = \frac{1}{\mu_d}\left[\left(\sqrt{2\dot{\varepsilon}_{ij}^{I}\Lambda_{ijkl}\dot{\varepsilon}_{kl}^{I}}\right)^{\frac{1}{n_d}} - \frac{1}{Y_o}\right] \end{aligned} \tag{7}$$

Note in the above state, flow and evolution equations, the various stress components and material functions are defined as follows:

$$q_{ij} = \sum_{a=1}^{M} q_{ij}^{(a)}, \qquad \alpha_{ij} = \sum_{b=1}^{N} \alpha_{ij}^{(b)} \tag{8}$$

$$\Gamma_{ij} = \Lambda_{ijkl}\left(\sigma_{kl} - \alpha_{kl}\right), \qquad \pi_{kl}^{(b)} = \Lambda_{ijkl}\alpha_{ij}^{(b)} \tag{9}$$

$$f(F) = \frac{F^n}{2\mu} \tag{10}$$

$$g\left(G^{(b)}\right) = H_{(b)}\left\langle 1-\sqrt{G^{(b)}}\right\rangle^{\beta_{(b)}} \tag{11}$$

and

$$F = \frac{1}{2\kappa^2}\left(\sigma_{ij}-\alpha_{ij}\right)\Lambda_{ijkl}\left(\sigma_{kl}-\alpha_{kl}\right)-1 \tag{12}$$

$$G^{(b)} = \frac{1}{2\kappa_{(b)}^2}\left(\alpha_{ij}^{(b)}\Lambda_{ijkl}\alpha_{kl}^{(b)}\right) \tag{13}$$

Furthermore, all three fourth-order viscoelastic moduli tensors, $E_{ijkl}$, $M_{ijkl}$ and $\eta_{ijkl}^{(a)}$, are taken to be coaxial, that is, $E_{ijkl} = E_s N_{ijkl}$, $M_{ijkl}^{(a)} = M_{(a)} N_{ijkl}$, and $\eta_{ijkl}^{(a)} = \rho_a M_{ijkl}^{(a)}$

where

$$N_{ijkl} = \left\{\frac{\nu}{(1+\nu)(1-2\nu)}\delta_{ij}\delta_{kl} + \frac{1}{(1+\nu)}\left(\delta_{ik}\delta_{jl}+\delta_{il}\delta_{jk}\right)\right\}$$

A key feature of the current GVIPS constitutive model, as opposed to more traditional plasticity and viscoplasticity types of approaches that have been applied to the analysis of metals, is that in the GVIPS formulation, the total strain ($\varepsilon_{ij}$) is partitioned into reversible ($\varepsilon_{ij}^{ve}$) and irreversible ($\varepsilon_{ij}^{vp}$) regimes and the stress is partitioned into equilibrium ($\sigma_s$, and $\left(\sigma_{ij}-\alpha_{ij}\right)$) and non-equilibrium components ($q_{ij}^{(i)}$ and $\alpha_{ij}^{(i)}$), as shown in Figure 7.

In general, previous models assumed the reversible or "elastic" regime to be time-independent and the irreversible strains were considered to be either time-independent ("plastic"), or more commonly time-dependent ("viscoplastic"). Recent research efforts have determined that strains in the reversible regime can be both time-independent and time-dependent (Saleeb and Arnold, 2001; Arnold et al., 2001) depending on the temperature. Therefore concepts from viscoelasticity, which previously had not been applied to metals, actually need to be applied to the constitutive equations employed to analyze metals. Furthermore, in the regime of time-dependent strains, due to the wide spectrum of rate-dependence of the material in both the reversible and irreversible domains, multiple mechanisms (spring-dashpot sets in terms of the mechanical analogues, see Figure 7) need to be included. The more mechanisms that are used, the more likely the characterized model is to appropriately model the behavior across all strain rates. Obviously, the more mechanisms that are present, the more model parameters and experiments, which isolate these various mechanisms are required, so judgment has to be employed in choosing the number of mechanisms.

Recently, the GVIPS model was extended to include damage to account for the softening due to stiffness and/or strength-reduction mechanisms present in the material (Saleeb and Wilt, 2005). It is this feature of the model, when linked with state-awareness capabilities, which will provide the required ability of the prognostic model to compute the damage progression and ultimate life in a structure.

## 4 CHARACTERIZATION OF GVIPS MODEL

Now, given fundamental material response histories, the most important, and often times most difficult[†] aspect of modeling the behavior of a given material is obtaining the required material functions (e.g., f(F) and g(G)) and associated material parameters, see Eq. (12) and Eq. (13). The difficulty associated with this process typically stems from not only the variety in mathematical forms for the material functions (e.g., power law, exponential, hyperbolic sine, etc.), but also given the material functions, there is often no unique set of material parameters for any given load path. Therefore, numerous iterations and difficult compromises are required before a final set of material parameters (for the assumed material functions) can be obtained.

Traditionally, characterization has been accomplished through basic trial and error procedures (i.e., graphical and/or mechanistic) which attempt to fit the predicted response from the constitutive model to that response exhibited by the experimental test data. In the case of idealized elastic, elastic-plastic or steady state creep material behavior; these approaches are quite successful; however for more general and sophisticated constitutive models, they are rather limited, difficult, and many times less than fruitful. This is particularly true when dealing with models that possess a very large number[‡] of material constants (such as the GVIPS model) that: (i) are often lacking in their direct physical interpretation (this is not the case in the GVIPS model), (ii) may have vastly different magnitudes, and (iii) are highly interactive. Further complications arise when a large number of experimental tests of various types (i.e., stress-, strain-, or mixed-control) under transient and/or steady-state

[†] Depending upon the sophistication of the constitutive model and environment; e.g. room temperature versus elevated temperature and loading conditions

[‡] In the specific model presented, the total number of material parameters required is 9 +9N + 2M where N defines the number of viscoplastic mechanisms and M the number of viscoelastic.

conditions, are expected to be simulated. Thus there is an obvious need for a systematic development of a general methodology for constitutive parameter estimation. Recently, software tools have been developed (e.g., *COMPARE* (Saleeb et al., 2002; Saleeb, et al., 2004) *and Z-mat* (Z-mat, 2006)) to enable a design engineer to easily and efficiently bridge the gap between constitutive theory and experimental test data. Optimum material parameters are determined by minimizing the errors between experimental data and the correlated responses. Within *COMPARE* the estimation of material parameters is accomplished by casting the problem as a minimum-error, weighted least-squares, multi-objective optimization problem; wherein, this optimization problem is solved using the Sequential Quadratic Programming Technique. Also, *COMPARE* is sufficiently general to handle a comprehensive set of test data, under arbitrary load-control variables, multiaxial stress/strain state, and transient as well as steady-state response measurements. Figure 8 shows a schematic flowchart of the process COMPARE uses to obtain the required parameters.

It is important to realize from the outset, that the resulting set of material parameters (regardless of the parameter estimation tool used to obtain them) is non-unique (due to the nonlinear nature of the problem), however if a sufficient amount of "data content" is provided then it is generally believed that the final obtained parameters should be relatively independent of the initial guess and bounds provided. Here data content is meant to imply not just quantity but also variety of experimental data; which will highlight and illuminate various issues such as multiaxiality, time scale, control mode (stress versus strain) and multiple deformation and damage mechanisms, to name a few. For example in the case of time scales, if one only provided stress-strain tensile data then one should not expect a model, that possesses sufficient breadth, to be able to accurately predict both creep and relaxation response; since the time duration of these types of tests far exceeds that of a tensile test. Similarly, if one provides only creep or relaxation data, one should not expect the model to accurately represent the typically shorter time domain tensile behavior of a given material (Arnold, 2006).

## 5 CHARACTERIZATION RESULTS

To demonstrate the ability of the GVIPS model to simulate the full range of the deformation and damage response of advanced metallic materials, the viscoelastoplastic behavior of an advanced titanium alloy, Ti-6Al-4V (commonly referred to as Ti-6-4), is being investigated. The characterization process is only partially complete for the deformation response and is

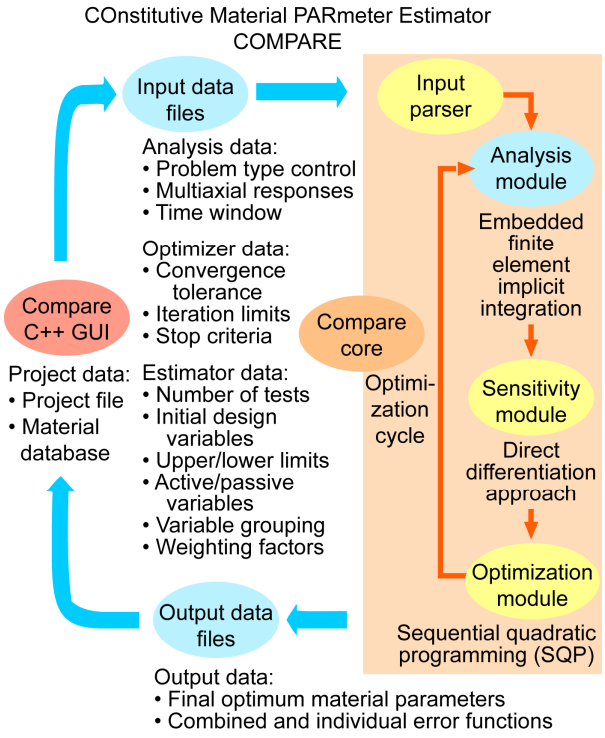


Figure 8: Flow chart for COMPARE software.

currently incomplete for the damage response (which is admittedly the portion of most significance for the development of prognostics tools). However, even the efforts which have been completed to date provide insight into the complexity of the material response of this alloy, and how the elevated temperature response of this material has characteristics which are not normally accounted for in classical methods of materials analysis, but which can be accounted for by using the GVIPS model. Ti-6-4 is an alpha-beta titanium alloy, represents the salient features of a class of materials (titanium) to be used in such targeted applications as compressor blades, disks, etc., and represents over 50% of all titanium to be used in jet engine components. Therefore its selection enables the appropriate physics-of-failure to be studied, incorporated and validated within the GVIPS prognosis model. After examining the literature for deformation and life data, numerous holes in the material characterization database (both with respect to reversible and irreversible behavior) for Ti-6-4 existed, thus necessitating an extensive amount of deformation and damage testing (of which approximately 65% is complete) and analysis to be conducted.

The need for an advanced viscoelastoplastic model to analyze the deformation response of Ti-6-4 at elevated temperatures is demonstrated in Figure 9, where the variation of the moduli and threshold stress ($\kappa$) (delineates the reversible and irreversible strain

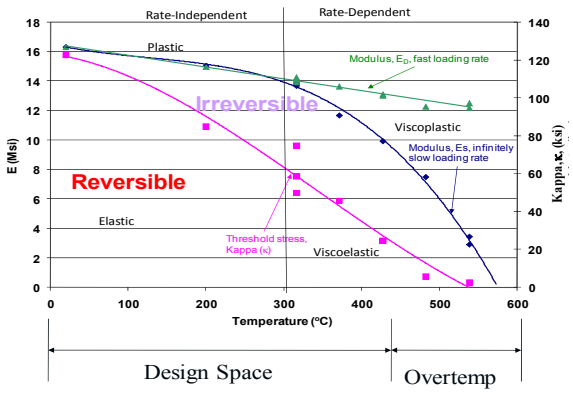


Figure 9: Variation of modulus and threshold stress as a function of temperature for Ti-6-4 material.

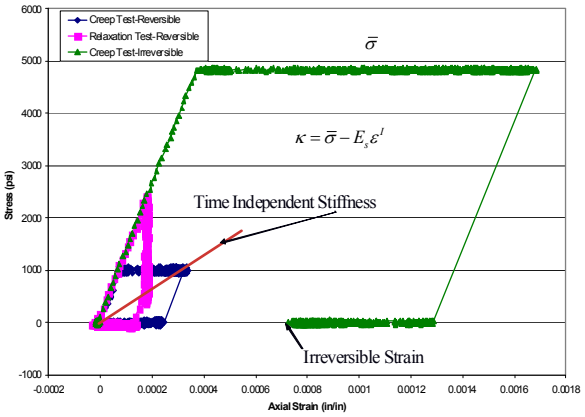


Figure 10: Determination of threshold stress and time-independent stiffness for GVIPS model.

regimes) are plotted as a function of temperature in Figure 9. The modulus $E_S$ represents the "infinitely slow" modulus, i.e. the elastic modulus of the material if it was loaded at an infinitely slow strain rate, whereas the modulus $E_D$ represents the "dynamic modulus",

$$E_D = E_S + \sum_{a=1}^{N} M_{(a)} \tag{14}$$

which is the modulus of the material, if it is loaded at an "infinitely fast" (i.e., very high, $1x10^{-3}$) rate. As can be seen in Figure 9, at elevated temperatures there is a significant difference between the two modulus values, indicating that even in the so-called "elastic" range, there is significant time-dependence. Below a temperature of about 300 °C, the two moduli are approximately equal, indicating the response of the Ti-6-4 material is rate-independent yet not necessarily time-independent. Above this temperature, the response is rate-dependent and time-dependent. To appreciate the practical significance of this fact, the operating temperatures typically encountered in aircraft engines are also noted below the horizontal axis in Figure 9, as well as the occasional, higher-temperature regime encountered during over-temp maneuvers. Clearly, even when one is within the typical engine design range and expecting the material response to be reversible, or "elastic", the materials behavior (at least in the case of Ti-6-4) would in fact be rate-dependent and would deform an additional $\sigma^*/E_s$ amount of strain over time, where $\sigma^*$ is the current applied stress. Consequently, at stresses below κ, if classical elasticity methods were used in the design, then this rate dependence, i.e., viscoelastic response, would not be captured. Furthermore, at stresses above κ, the material response is viscoplastic due to the rate-and-time-dependence, and similarly using the classical methods of plasticity in analysis and design, would also not be accurate.

Figure 9 further indicates that the value of the threshold stress, κ, decreases significantly as a function of temperature. While not shown here, the important point to note is that at elevated temperatures the threshold stress (κ) is significantly below the traditional "proportional limit" or "yield stress" of the material. This factor then leads to the conclusion that irreversible material behavior takes place at stress levels well below those considered using traditional methods for the analysis of metals. If classical design methods were used, the material response below the "proportional limit" would be assumed to be fully reversible, and only the response after the proportional limit would be assumed to be irreversible. However, as is shown in the figure, that assumption could lead to significant inaccuracies in the predictions of the material response.

The modulus $E_s$ can be determined from a creep test and a relaxation test conducted within the reversible regime, as demonstrated in Figure 10. In this figure, results from two creep tests (one below κ and one above) and a relaxation test are shown on the same stress-strain plot. Note, the points where the creep and relaxation cease (thus indicating an equilibrium state) are connected and the slope of the resulting line can be considered to be the time independent stiffness, $E_s$. The value of the threshold stress κ can be computed by a process known as "viscoelastic subtraction" [Arnold et al, 2001]. In this procedure, a creep test is conducted well below κ (estimated for example by taking a stress level 50% below the proportional limit resulting from a slow-rate tensile test (e.g., $1x10^{-6}$ or less)), and after the creep stops, the material is unloaded and then held at zero stress or strain until all of the strain or stress is recovered. If the creep stress is in the "irreversible" range of the material response, after a period of time

being held at zero stress the strain recovery will cease, leaving an inelastic (irreversible) strain. The value of the threshold stress can then be computed by using the value of this creep stress, the inelastic strain obtained, and the time-independent stiffness $E_s$ (see the equation in Figure 10).

Repeating this procedure for each temperature, the viscoelastic behavior of the material (Ti-6-4) can be characterized across a range of temperatures. In this case, Table 2 shows the resulting characterized material constants for Ti-6-4 from 371 °C to 538 °C. The variation of the parameters with temperature is shown schematically in Figure 11.

Table 2: Characterized viscoelastic material constants for Ti-6-4 material

| Temp, °C: | 371 | 427 | 482 | 538 |
|---|---|---|---|---|
| $E_s$ (psi): | 10,687,600 | 8,890,370 | 7,037,810 | 2,444,950 |
| $M_1$ (psi): | 110,887 | 499,594 | 736,202 | 1,399,370 |
| $\rho_1$ (1/s): | 700 | 200 | 38 | 31 |
| $M_2$ (psi): | 1,200,000 | 1,453,840 | 1,722,430 | 2,133,740 |
| $\rho_2$ (1/s): | 9,580 | 622 | 338 | 250 |
| $M_3$ (psi): | 931,104 | 1,299,240 | 1,586,740 | 2,064,350 |
| $\rho_3$ (1/s): | 55,086 | 6,085 | 1,024 | 882 |
| $M_4$ (psi): | 580,000 | 959,668 | 1,276,920 | 1,797,670 |
| $\rho_4$ (1/s): | 110,000 | 60,031 | 6,731 | 3,000 |
| $M_5$ (psi): | | | 291,605 | 1,345,300 |
| $\rho_5$ (1/s): | | | 20,000 | 12,643 |
| $M_6$ (psi): | | | | 1,097,820 |
| $\rho_6$ (1/s): | | | | 85,187 |

The value of the Maxwell mechanism, spring moduli ($M_{(i)}$) increases linearly with temperature, indicating that the viscoelastic response and time-dependence increases with increasing temperature. Conversely, the characteristic relaxation time ($\rho_a$, a = 1 to M) decreased in a parabolic fashion with temperature, indicating that the level of transient response increased as the temperature was increased.

As discussed earlier, the value of the time-independent stiffness ($E_s$) also decreased parabolically, but unlike with the relaxation time, the rate of decrease was higher at higher temperatures. As can be observed in Table 2, the number of mechanisms required to characterize the material increased with temperature, as well. This result suggests that the amount of reversible time-dependence in the material response increased with increasing temperature.

The overall characterization of the viscoelastic material response for Ti-6-4 has thus far been very successful. Figure 12 shows experimental and computed stress-strain results from a representative creep test and a representative relaxation test conducted at 538 °C, below κ. For the creep test, the creep response (including creep shutdown), unload, and strain recovery at zero load were all well correlated. The

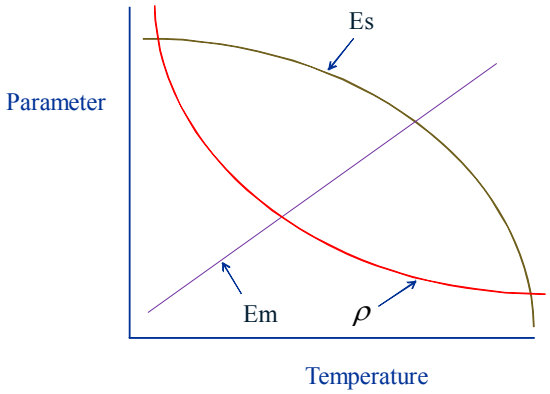


Figure 11: Variation of viscoelastic parameters with temperature.

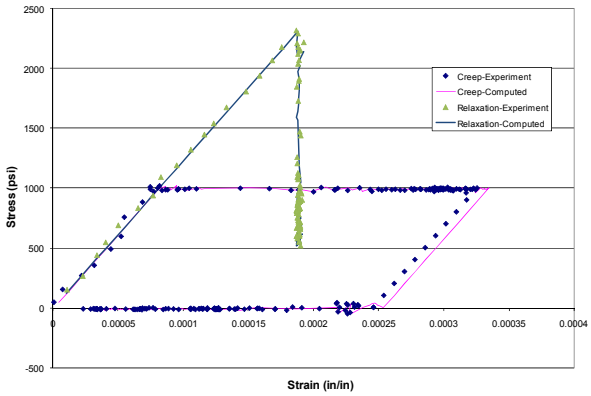


Figure 12: Correlation of viscoelastic creep and relaxation response of Ti-6-4 at 538 °C.

relaxation response (including relaxation shutdown) was also well correlated. Figure 13 shows a normalized plot of the experimental and computed stress-time response resulting from relaxation tests conducted at several temperatures. The temperature dependence of the relaxation response was captured, and the overall quantitative correlation between the experimental and computed results was reasonable. These results all indicate that the GVIPS model can simulate the time-dependent reversible deformation response of metallic alloys.

To characterize the viscoplastic (irreversible) portion of the material response, a series of creep and relaxation tests have been initiated. The deformation test program thus far completed is summarized in Table 3. A series of relaxation tests were conducted at temperatures ranging from room temperature (20 °C) to 538 °C. The relaxation tests were carried out at a variety of strain rates. Thus, the interaction of the strain rate-dependence, time and temperature-dependence of the material could be quantified. The expected temperature-dependence of the various viscoplastic material parameters is shown schematically in Figure 14.

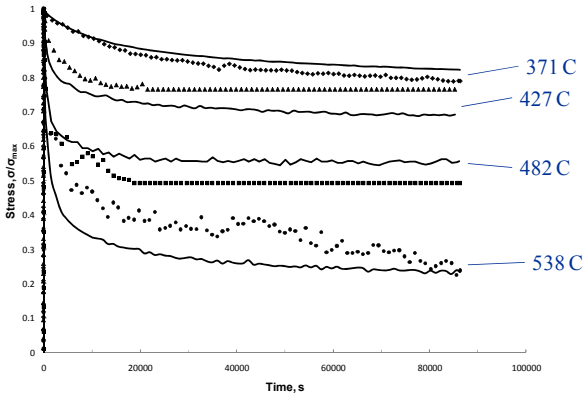


Figure 13: Correlation of viscoelastic relaxation stress-time response at various temperatures for Ti-6-4.

Table 3: Test matrix to characterize the irreversible material response of Ti-6-4 material.

| Test type | Temperature ( C) | Strain rate (1/s) | strain level (in/in) | stress level (ksi) |
|---|---|---|---|---|
| relaxation | 20 | 0.0000006 | 0.018 | |
| relaxation | 20 | 0.001 | 0.018 | |
| relaxation | 200 | 0.0000006 | 0.018 | |
| relaxation | 200 | 0.001 | 0.018 | |
| relaxation | 316 | 0.0000006 | 0.018 | |
| relaxation | 316 | 0.00099 | 0.018 | |
| creep | 316 | 0.00101 | | 75 |
| creep | 316 | 0.00101 | | 81 |
| creep | 316 | 0.00103 | | 85 |
| relaxation | 371 | 0.0000006 | 0.018 | |
| relaxation | 371 | 0.00099 | 0.018 | |
| creep | 371 | 0.001 | | 75 |
| relaxation | 427 | 0.0000006 | 0.006 | |
| relaxation | 427 | 0.0000006 | 0.018 | |
| step relaxatior | 427 | 0.0000006 | .006, .012 | |
| relaxation | 427 | 0.0000008 | 0.006 | |
| relaxation | 427 | 0.0000008 | 0.006 | |
| relaxation | 427 | 0.0000008 | 0.018 | |
| step relaxatior | 427 | 0.0000008 | .006, .012, .018 | |
| step relaxatior | 427 | 0.0000008 | .012, .018 | |
| relaxation | 427 | 0.0000099 | 0.018 | |
| relaxation | 427 | 0.00001 | 0.018 | |
| relaxation | 427 | 0.000099 | 0.018 | |
| relaxation | 427 | 0.0001 | 0.018 | |
| creep | 427 | 0.000977 | | 70 |
| relaxation | 427 | 0.001 | 0.018 | |
| relaxation | 427 | 0.001 | 0.018 | |
| steprelaxation | 427 | 0.001 | .006, .012, .018 | |
| step relaxatior | 427 | 0.001 | .006, .018 | |
| step relaxatior | 427 | 0.001 | .012, .018 | |
| creep | 427 | 0.001037 | | 65 |
| creep | 427 | 0.001039 | | 55 |
| creep | 427 | 0.0024 | | 75 |
| relaxation | 482 | 0.0000006 | 0.018 | |
| relaxation | 482 | 0.00099 | 0.018 | |
| relaxation | 538 | 0.0000006 | 0.006 | |
| relaxation | 538 | 0.0000006 | 0.018 | |
| relaxation | 538 | 0.0000006 | | |
| relaxation | 538 | 0.001 | 0.018 | |
| creep | 538 | 0.0011 | | 55 |
| creep | 538 | 0.0011 | | 15 |
| creep | 538 | 0.0012 | | 35 |
| Modulus | various | various | ±0.001 | |

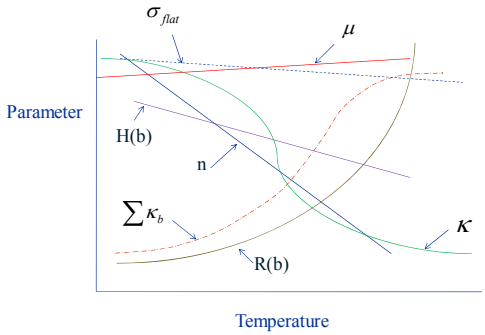


Figure 14: Variation of viscoplastic parameters with temperature.

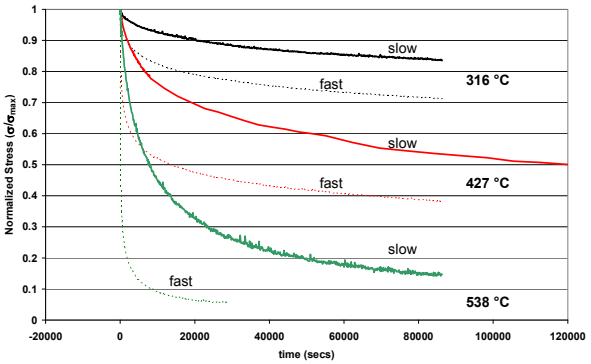


Figure 15: Effect of strain rate and temperature on viscoplastic relaxation response for Ti-6-4 material.

Test results obtained to date demonstrate the rate-time- and history-dependence of the material response. These results show that advanced, multimechanism, viscoelastoplastic models are required to model the details of the material response. Traditional modeling methods are incapable of capturing the complex phenomena observed in the deformation response of metals at high temperature. For example, in Figure 15 the normalized stress-time plots from relaxation tests conducted at various temperatures at slow ($6x10^{-7}$ /s) - and fast (0.001 /s) -loading strain rates are shown. As can be seen in the figure, there is a noticeable strain rate dependence of the material response, and the rate-dependence increases with increasing temperature. These results also suggest the need for at least two, if not more, viscoplastic mechanisms since the material response given only a single mechanism would show identical relaxation response even when loaded at different initial strain rates.

A series of relaxation and step relaxation tests were conducted at 427 °C which included a pure relaxation test in which the material was loaded to 1.8% strain and relaxed for 24 hours; a two-step relaxation test where the material was loaded to 1.2% strain, relaxed for

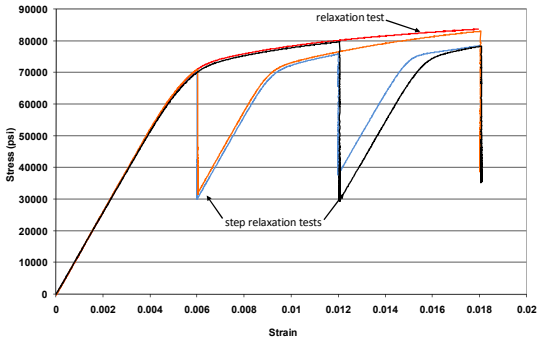


Figure 16: Stress-strain results from relaxation and step relaxation tests conducted at 427 °C to demonstrate history dependence of viscoplastic behavior.

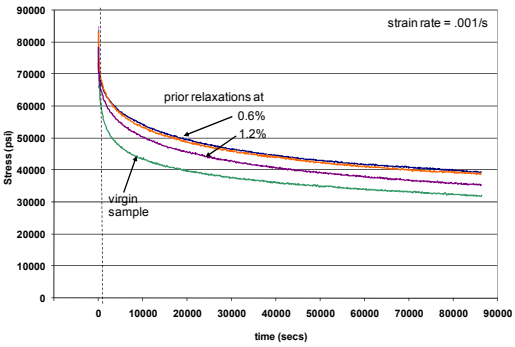


Figure 17: Stress-time results for relaxation at 1.8% strain from relaxation and step relaxation tests conducted at 427 °C to demonstrate history dependence of viscoplastic behavior.

24 hours, and then reloaded to 1.8% strain where the material was relaxed again; a two-step relaxation test where the material was loaded to 0.6% strain, relaxed, reloaded to 1.8% strain and relaxed; and finally a multi-step test where the material was loaded to 0.6% strain, relaxed, loaded to 1.2% strain and relaxed, and finally loaded to 1.8% strain and relaxed. Stress-strain curves from these tests are shown in Figure 16, and the corresponding stress-time curves (taken from the relaxation portion which took place at 1.8% strain) for each of these tests are shown in Figure 17. The stress-strain curves show that the prior history (i.e., step relaxation) did not largely affect the overall stress-strain response, as upon reloading the material trended towards the original stress-strain curve. However, the stress-time curves, shown in Figure 17, do demonstrate the history-dependence of the material, as the relaxation response varied based on the prior stress relaxations.

Standard creep tests were also conducted at several temperatures and stress levels. Although not shown in the test matrix displayed in Table 3, step-creep and

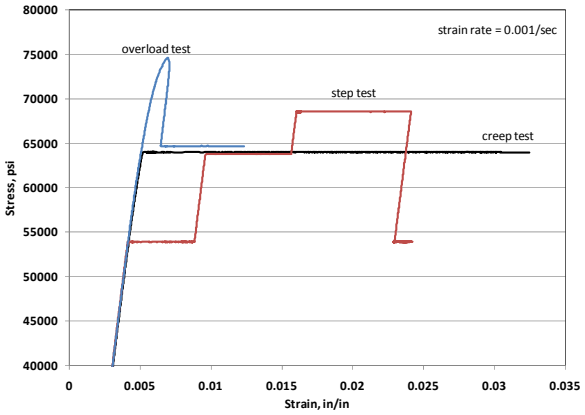


Figure 18: Stress-strain curves of creep, step creep and creep overload tests at 427 °C.

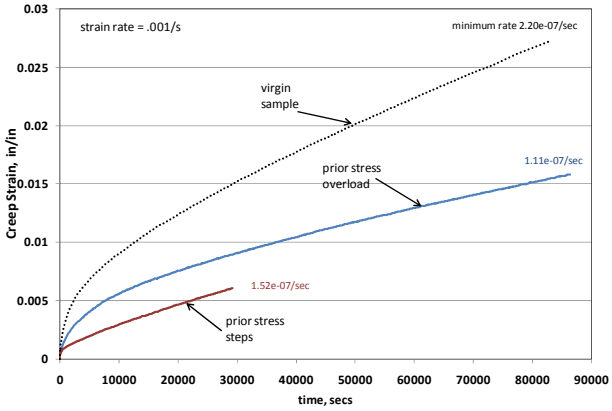


Figure 19. Strain vs. time results from creep tests conducted at 65 ksi and 427 °C to demonstrate history dependence of viscoplastic material behavior.

creep-overload tests were also conducted to quantify the history-dependence of the material, as well as the "creep-plasticity" interaction. Figure 18 shows stress-strain curves from the various types of creep tests that were conducted at 427 °C. The step-creep tests serve to demonstrate the history-dependence of the material response. The creep overload test shown in Figure 18, in which the material is loaded to a 75 ksi stress level, then unloaded to 65 ksi stress level and crept as compared to a "virgin" creep curve conducted at 65 ksi level, serves to demonstrate the "creep-plasticity" interaction observed in metals, and in particular Ti-6-4. Phenomena of this type cannot be simulated using classical time-independent plasticity coupled with time-dependent creep analysis methods. Figure 19 shows the corresponding strain-time curves for the standard creep, step-creep and creep-overload tests generated from creeping at a stress level of 65 ksi. As can be seen in the figure, the creep response of the material is strongly dependent on the material's prior history before the creeping (constant load portion of the history) took

place. It is precisely this creep-plasticity interaction phenomenon that demanded, decades ago, the development of "unified" viscoplastic models (like the current GVIPS formulation) to accurately capture this type of behavior. The term unified implies that only a single inelastic strain (which captures both time-dependent and time-independent behavior) is included in the constitutive model. Overall, titanium alloys demonstrate a full range of rate- and time-dependent material response over a wide stress and temperature range. The goal of the project will be to characterize this full range of material behavior using the GVIPS model. Ongoing work includes the characterization of the viscoplastic portion of the GVIPS model as well as the measurement and characterization of the influence of damage mechanisms on the mechanical response of Ti-6-4. These results will be documented in future publications.

## 6 CONCLUSIONS

A novel, integrated prognostic model (with linkages to diagnostics methods) has been proposed for structural health monitoring, with particular applicability to hot engine structures. The key requirements for prognostics methods, and a general discussion of how these methods can be linked with diagnostics techniques, have been discussed, as well as an experimental approach for fully exploring and validating the proposed methodology. The necessity of including an advanced multi-mechanism viscoelastoplastic model as a key component of the prognosis methodology has been demonstrated. To provide a prognosis method that is not just an extrapolation of previously observed material behaviors, advanced constitutive models are required which can be linked to the diagnostic methods through state-awareness techniques. As engine structures will encounter elevated temperatures, classical analysis methods and constitutive equations will not be able to accurately simulate all of the features of the material response. Therefore, the advanced GVIPS viscoelastoplastic constitutive model will be of significant use as a true prognosis tool. To partially demonstrate the ability of the prognostics tool to simulate advanced features of the material response of metallic alloys, results obtained from the characterization of the reversible portion of the material model for a representative titanium alloy (i.e., Ti-6-4) have been presented. Furthermore, a description of the test program that is being conducted to characterize the irreversible portion of the constitutive model, along with some representative results, which demonstrate the full history-dependence of the material response has been discussed. Future efforts will involve fully characterizing the irreversible portion of the material model both uniaxially and biaxially, as well as carrying out a coupled experimental/analytical study to characterize the damage portions of the material behavior. This method will then be linked to appropriate diagnostic methods through state-awareness systems to provide a full-featured structural health monitoring system.

## NOMENCLATURE

### Invariants

| | |
|---|---|
| $\Omega$, $\Omega_R\Omega_{IR}$ | Complementary dissipation potential; *R*-reversible, *IR*-irreversible |
| $\Phi$, $\Phi_R$ $\Phi_{IR}$ | Gibb's complementary potential; *R*-reversible, *IR*-irreversible |
| $F$ | Bingham-Prager threshold function |
| $G^{(b)}$ | Normalized second invariant function |

### Stresses

| | |
|---|---|
| $\sigma_{ij}$ | Applied Cauchy stress tensor |
| $(\sigma_s)_{ij}$ | Viscoelastic equilibrium stress tensor |
| $\sigma_{ij}$ - $\alpha_{ij}$ | Viscoplastic equilibrium stress tensor |
| $q_{ij}, q_{ij}^{(a)}$ | Viscoelastic non-equilibrium internal stress |
| $\alpha_{ij}, \alpha_{ij}^{(b)}$ | Viscoplastic non-equilibrium internal stress |
| $\kappa$ | Drag stress, flow threshold parameter delineating the reversible from irreversible domain |
| $\kappa_{(b)}$ | Either a normalizing stress or hardening threshold stress per mechanism |

### Strains

| | |
|---|---|
| $\varepsilon_{ij}$ | Total strain |
| $\varepsilon_{ij}^{ve}$ | Reversible mechanical strain |
| $\varepsilon_{ij}^{I}$ | Irreversible mechanical strain (inelastic/ viscoplastic) |
| $\varepsilon_{ij}^{th}$ | Thermal strain |
| $p_{ij}$ | internal reversible strain tensor (displacement-like) |
| $\gamma_{ij}$ | internal irreversible strain tensor |

### Material Parameters

| | |
|---|---|
| $E_{ijkl}, M_{ijkl}^{(a)}, \eta_{ijkl}^{(a)}$ | Reversible elastic stiffness, viscoelastic stiffness and viscosity coefficient tensor for the $a^{th}$ mechanism, respectively |
| $E_s, E_m^{(a)}$ | Denotes the elastic stiffness and maxwell spring stiffness per $a^{th}$ mechanism, respectively |

| | |
|---|---|
| $E_d$ | Dyanmic Modulus |
| | Poisson Ratio |
| | Stiffness per Maxwell mechanism a |
| $\rho_a$ | Relaxation spectrum per $a^{th}$ mechanism; $= E_\eta^{(a)} / E_m^{(a)}$ |
| $\mu$ | material parameter associated with irreversible viscosity of the material. |
| n, $\beta_{(b)}$, | $m_{(b)}$ material exponents |
| $H_{(b)}$, $R_{(b)}$, | Hardening and Thermal recovery parameters per mechanism |
| $c_e, \overline{Y}_0, \mu_e, n_e$ | Stiffness reduction parameters |
| $\Psi$ | stiffness reduction parameter |
| $c_d^{(i)}, Y_0^{(i)}, \mu_d^{(i)}, n_d^{(i)}$ | Strength reduction parameters |
| *f(F), r($G^{(b)}$)* | material functions |

**Miscellaneous**

| | |
|---|---|
| $\Lambda_{ijkl}$ | Devatoric operator (isotropic or anisotropic) |
| $N_{ijkl}$ | Isotropic directionality tensor |
| $\delta_{ij}$ | Kronecker delta function |
| $(\dot{x})$ | time derivative (or rate) notation |
| $\langle\ \rangle$ | Macauley bracket |
| M | Number of reversible mechanisms |
| N | Number of irreversible mechanisms |
| T | Temperature |

**REFERENCES**


(Adams, 2004) D.E. Adams. "Diagnosis and Prognosis in Structural Systems", A short course, Ohio Aerospace Institute, 2004.

(Arnold et al, 2001) S.M. Arnold, A.F. Saleeb, M.G. Castelli. ''A General Reversible Hereditary Constitutive Model: Part II Application to Titanium Alloys", JEMT, Vol. 123, pp. 65-73, 2001.

(Arnold, 2006) S.M. Arnold. "Paradigm Shift in Data Content and Informatics Infrastructure Required for Generalized Constitutive Modeling of Materials Behavior", MRS Bulletin, December, pp. 1013-1021, 2006.

(Dowling, 1999) N.E. Dowling. Mechanical Behavior of Materials: Engineering Methods for Deformation, Fracture, and Fatigue, Prentice Hall, New Jersey, 1999.

(Fatemi and Yang, 1998) A. Fatemi and L. Yang. "Cumulative Fatigue damage and life prediction theories: a survey of the state of the art of homogeneous materials", Int. J. of Fatigue, Vol. 20, No.1, pp. 9-34, 1998.

(Grandt, 2004) A.F. Grandt. "Fundamentals of Structural Integrity", John Wiley & Sons, 2004.

(Hess, 2002) A. Hess. "The Prognostic Requirement for Advanced Sensors and Non-Traditional Detection Technologies", DARPA/DSO Prognosis Bidder's Conference, Alexandria, Va, 2002.

(Lemaitre and Chaboche, 1990) J. Lemaitre and J.L. Chaboche. Mechanics of Solid Materials, Cambridge University Press, 1990.

(MDMC, 2006) MDMC. www.mdmc.net, Cambridge, United Kingdom, 2006.

(Odqvist, 1936) F. Odqvist. Theory of Creep Under the Action of Combined Stresses with Applications to High Temperature machinery", Proc. Royal Swedish Institute for Engineering Research, N. 141, 1936.

(Rytter, 1993) A. Rytter, "Vibration based inspection of civil engineering structures," Ph. D. Dissertation, Department of Building Technology and Structural Engineering, Aalborg University, Denmark, 1993.

(Saleeb and Wilt, 1993) A.F. Saleeb, and T.E. Wilt. "Analysis of the Anisotropic Viscoplastic Damage Response of Composite Laminates - Continuum Basis and Computational Algorithms." *International Journal for Numerical Methods in Engineering*, 36(10), pp. 1629, 1993.

(Saleeb, et al, 2001) A.F. Saleeb, S.M. Arnold, M.G. Castelli, T.E. Wilt, and W.E. Graf. "A General Hereditary Multimechanism-Based Deformation Model With Application to The Viscoelastoplastic Response of Titanium Alloys, Int. Jnl. Of Plasticity, Vol. 17, No. 10, pp. 1305-1350, 2001.

(Saleeb and Arnold, 2001) A.F. Saleeb, and S.M. Arnold. ''A General Reversible Hereditary Constitutive Model: Part I Theoretical Developments", JEMT, Vol. 123, pp. 51-64, 2001.

(Saleeb, et al, 2002) A.F. Saleeb, A.S. Gendy, T.E. Wilt. "Parameter-Estimation Algorithms For Characterizing A Class of Isotropic and Anisotropic Viscoplastic Material Models", Int. Jnl. of the Mechanics of Time Dependent Materials, Vol. 6, No. 4, pp. 323-361, 2002.

(Saleeb and Arnold, 2004) A.F. Saleeb and S.M. Arnold. "Specific Hardening Function Definition and Characterization of A Multimechanism Generalized Potential-Based Viscoelastoplasticity Model", *Int. Jnl of Plasticity*, Vol. 20, pp. 2111-2142, 2004.

(Saleeb, et al, 2004) A.F. Saleeb, J.R. Marks, T.E. Wilt, and S.M. Arnold. "Interactive Software for Material Parameter Characterization of Advanced Engineering Constitutive Models", Adv. Eng. Software, Vol. 35, pp. 383-398, 2004.

(Saleeb and Wilt, 2005) A.F. Saleeb, and T.E. Wilt. On Extending the Capabilities of COMPARE to Include

Material Damage, NASA CR-2005-213815, 2005.

(Saleeb and Ponnaluru, 2006) A.F. Saleeb, and G.K. Ponnaluru. Enhancement of the Feature Extraction Capability in Global Damage Detection Wavelet Theory, NASA CR-2006-21225, May 2006.

(Saleeb and Prabhu, 2002) A.F. Saleeb, and M. Prabhu. Defect Localization Capability of a Global Detection Scheme: Spatial Pattern Recognition Using Full-Field Vibration Test Data in Plates, NASA CR-2002-211685, Aug 2002.

(Skrzypek and Hetnarski, 2000) J. Skrzypek and R. Hetnarski. Plasticity and Creep, Theory, Examples, and Problems, CRC Press, 2000.

(Springer, 2004) Springer, JOM, Volume 56, Issue 3, 2004.

(Z-mat, 2006) Z-mat Library, http:// www.nwnumerics.com/Z-mat/, Seattle, WA, 2006.